$P2Y_2$ Receptor Agonist INS37217 Enhances Functional Recovery after Detachment Caused by Subretinal Injection in Normal and *rds* Mice

May Nour,[1] *Alexander B. Quiambao,*[2] *Ward M. Peterson,*[3] *Muayyad R. Al-Ubaidi,*[1,2] *and Muna I. Naash*[1,2]

Purpose. To evaluate the effects of INS37217 on the recovery of retinal function after experimental retinal detachment induced by subretinal injection.

Methods. Subretinal injections of 1 μL of fluorescent microbeads, saline, or INS37217 (1–200 μM) were made by the transvitreal method in normal (C57BL/6) mice and in mice heterozygous for the retinal degeneration slow (*rds*) gene. Control, mock-injected animals underwent corneal puncture without injection. Histologic and ERG evaluations were made at 0 to 1 and 8 hours, and 1, 3, 7, 10, 14, and 60 days post injection (PI). DNA fragmentation was evaluated by terminal deoxynucleotidyl transferase–mediated uridine 5′-triphosphate-biotin nick end labeling (TUNEL).

Results. A single subretinal injection of saline solution containing fluorescent beads caused a histologically evident retinal detachment and distributed the microbeads to almost all the subretinal space. Spontaneous reattachment occurred within 24 hours after injection and was accompanied by evident retinal folding that appeared largely resolved by 6 days later. Relative to controls, injection of saline resulted in approximately 40% recovery of dark-adapted a-wave amplitude at 24 hours PI and gradually improved to approximately 90% of controls at 2 months PI. Subretinal injection of saline containing INS37217 (10 μM) significantly increased rod and cone ERG of normal and $rds^{+/-}$ mice at 1 and 10 days PI, when compared with injection of saline alone. Additionally, INS37217 reduced the number of TUNEL-positive photoreceptors and the enhanced rate of reattachment.

Conclusions. Enhancement of ERG recovery by INS37217 is likely due to reduced retinal folding and cell death associated with detachment. These results support the use of INS37217 to help restore function after therapies that involve subretinal administration of drugs in animal models of retinal diseases.

From the [1]Oklahoma Center for Neuroscience and the [2]Department of Cell Biology, University of Oklahoma Health Sciences Center, Oklahoma City, Oklahoma; and [3]Inspire Pharmaceuticals, Durham, North Carolina.

Supported by Grant EY10609 (MIN) and Core Grant for Vision Research (EY12190 from the National Eye Institute; Inspire Pharmaceuticals, Inc.; the Foundation Fighting Blindness (MIN, MRA); and the Oklahoma Center for the Advancement of Science and Technology. MIN is a recipient of the Research to Prevent Blindness James S. Adams Scholar Award.

Submitted for publication May 12, 2003; revised June 9, 2003; accepted June 12, 2003.

Disclosure: **M. Nour**, None; **A.B. Quiambao**, None; **W.M. Peterson**, Inspire Pharmaceuticals (I, E); **M.R. Al-Ubaidi**, None; **M.I. Naash**, None

The publication costs of this article were defrayed in part by page charge payment. This article must therefore be marked "*advertisement*" in accordance with 18 U.S.C. §1734 solely to indicate this fact.

Corresponding author: Muna I. Naash, University of Oklahoma Health Sciences Center, 940 Stanton L. Young Boulevard, BMSB 781, Oklahoma City, OK 73104; muna-naash@ouhsc.edu.

(*Invest Ophthalmol Vis Sci.* 2003;44:4505–4514) DOI: 10.1167/iovs.03-0453

Retinal detachment disrupts the function and cellular organization of the retina, often resulting in severe and permanent visual loss in humans, even after successful reattachment. Histologically, some of the secondary effects of retinal detachment in experimental models include the proliferation of nonneuronal cells, hypertrophy of Müller cells, loss of proper morphologic organization, and photoreceptor cell death.[1–7] Many of these secondary effects are thought to occur as a result of detachment-induced hypoxia of photoreceptors, as well as disruption of vital photoreceptor and retinal pigment epithelium (RPE) interactions. These interactions are required for phagocytosis of photoreceptor outer segments,[8] metabolism and transport of vitamin A,[9–11] and the regulation of volume and composition of the subretinal space.[12,13] Retinal detachments in humans are usually treated with reattachment surgery, but successful anatomic retinal reattachment frequently does not correlate with restoration of normal visual function, especially in cases involving macular detachment.[14] Recovery of photoreceptor function has also been shown to lag dramatically behind retinal reattachment in animal models of induced retinal detachment. For example, in both clinical and experimental settings, recent studies have demonstrated a delay in the recovery of cone function after temporary retinal detachment.[15–17]

For many other types of vision-threatening diseases that also compromise photoreceptor function, a variety of investigative therapeutic interventions under preclinical assessment are contingent on inducing a temporary retinal detachment to deliver the therapeutic agent to the subretinal space. These diseases include the multisymptomatic and multifactorial inherited retinal degenerations (http://www.sph.uth.tmc.edu/RetNet/; provided in the public domain by the University of Texas Houston Health Science Center, Houston, TX).[18] Potential experimental therapies currently undergoing evaluation in animal models include pharmacological agents,[19,20] growth factors,[21–24] and viruses carrying therapeutic genes.[25–31] Subretinal injection represents perhaps the most accessible means of delivering some of these potential therapeutic agents to the photoreceptor and RPE, but also invariably results in the creation of a temporary retinal detachment.[32,33] Furthermore, subretinal injections of saline are currently conducted in patients with advanced age-related macular degeneration as part of a surgical technique called macular translocation surgery, which involves the creation of a retinal detachment to enable the surgeon to move the macula from a diseased region of the RPE to a healthier region.[34] Given the present and perhaps future practices of conducting subretinal injections as part of medical management of vision-threatening diseases, it is crucial to seek approaches that reduce the adverse effects of induced retinal detachment.

A pharmacological approach for enhancing reabsorption of extraneous subretinal fluid may help minimize some of the

adverse effects of naturally occurring and induced retinal detachments. Active and passive transport of ions and fluid across the RPE has been shown to play a major role in the regulation of subretinal fluid volume and composition.[35] Activation of appropriate fluid transport pathways in the RPE can therefore be targeted as a means of promoting retinal reattachment. For example, activation of $P2Y_2$ receptors located on the apical membrane of RPE cells using adenosine 5′-triphosphate (ATP) or uridine 5′-triphosphate (UTP) has been shown to stimulate ion transport and fluid absorption (apical-to-basolateral direction) in freshly isolated bovine RPE monolayers.[36,37] Synthetic $P2Y_2$ receptor agonists such as INS37217 or INS542 have also been shown to stimulate fluid reabsorption across bovine and human fetal RPE monolayers, enhance subretinal fluid reabsorption and retinal reattachment in rat and rabbit eyes, and increase active outward transport of fluorescein in rabbit eyes[38,39] (Maminishkis A, et al. *IOVS* 2000;41:ARVO Abstract 4541; Takahashi J, et al. *IOVS* 2002;43:ARVO E-Abstract 3265).

In the present study, we evaluated the recovery of retinal morphology and function after subretinal injections in the normal and $rds^{+/-}$ model for retinitis pigmentosa (RP). In addition, we assessed the effect of the synthetic $P2Y_2$ receptor agonist INS37217 on the recovery of retinal function after these subretinal injections. We report that the recovery of both rod and cone function lags behind morphologic reattachment and that INS37217 is able to enhance functional recovery in normal and $rds^{+/-}$ mice after retinal reattachment.

Materials and Methods

Animals

One-month-old normal C57BL/6 female mice (25–30 g) used in this study were bought from Harlan Sprague-Dawley Laboratories (Indianapolis, IN). For the mouse model of RP, $rds^{+/-}$ mice lacking one functional allele of the peripherin/*rds* (*Prph-2*) gene were used. Phenotypically, these mice display an early-onset loss of rod function, and a late-onset loss of cone function.[40] This electrophysiological dysfunction, as assessed by ERG is accompanied by a slow rate of photoreceptor cell loss. The gene defect of *rds* mice was first moved onto a pigmented background by continuous mating to normal C57BL/6 mice. The mice in the present study were generated from subsequent matings of $rds^{+/-}$ to normal (+/+) mice. The *rds* defect is inherited as a Mendelian trait, so that approximately half of the offspring were +/+ and half were $rds^{+/-}$. Mice were screened for the presence of the *rds* mutation by polymerase chain reaction amplification with two primers: MIN232 (5′-TGAGCCACAGCAGACGTTGG-3′) from the *Prph-2* gene intron I and MIN99 (5′- GACCCAGATTGCCTGTGGCA-3′) from the naturally occurring 9.2-kb inserted element in the mutant *rds* gene.[41] All mice studied were maintained in a breeding colony under cyclic light (12-hour light-dark) conditions; cage illumination was approximately 7 foot-candles during the light cycle. All experiments were approved by the local Institutional Animal Care and Use Committees, and conformed to the National Institute of Health Guide for the Care and Use of Laboratory Animals and the ARVO Statement for the Use of Animals in Ophthalmic and Vision Research.

Transvitreal Subretinal Injections

After anesthesia by an intramuscular injection of 85 mg/kg ketamine (Fort Dodge Animal Health; Fort Dodge, IA) and 14 mg/kg xylazine (The Butler Company; Columbus, OH) and before subretinal injection, the eyes were dilated with 2.5% phenylephrine (Akorn, Inc., Decatur, IL) and topically anesthetized with 0.5% proparacaine (Alcon Laboratories Inc., Fort Worth, TX). Animals were placed on a regulated heating pad, and images of the posterior pole were magnified under an operating microscope (model 212F; AusJena, Jena, Germany). After complete dilation was achieved, a drop of 2.5% methylcellulose was added to the corneal surface to visualize the fundus. A 28-gauge beveled hypodermic needle (BD Biosciences, Franklin Lakes, NJ) was used to puncture the cornea carefully, avoiding any contact with the lens. The transvitreal subretinal injections, previously described in rat,[42] were then performed with a 33-gauge blunt needle (Hamilton Co., Reno, NV). The blunt needle tip was inserted through the corneal puncture, across the vitreous and the shaft aimed at the back of the eyecup, avoiding any trauma to the lens or iris. A 1-μL volume of saline+fluorescein (0.1 mg/mL) or INS37217 (1–200 μM)+fluorescein (0.1 mg/mL) was injected into the subretinal space. Fluorescein was added to the injected material to visualize the injection, and bleb formation and was cleared from the eye as early as 4 hours post injection (PI). As a control for anesthesia, corneal puncture and erythromycin treatment, a group of animals underwent corneal puncture without subretinal injection. Subsequent to the injection, an erythromycin ophthalmic ointment (E. Fougera & CO, Melville, NY) was applied to the corneal surface to reduce the risk of infections and the associated opacifications. Animals injected with saline or fluorescent microbead solution (Fluoresbrite plain YG 1.0-μm microspheres; Polysciences, Inc., Warrington, PA) were then electrophysiologically and/or morphologically evaluated at 0 to 1, 8 hours, and 1, 3, 7, 10, 14, and 60 days PI. For each time point, an independent group of animals was analyzed. Side effects of the subretinal injection procedure include iris and subretinal bleeding (5%–10% incidence rate) which can contribute to either the persistence of retinal detachment or additional tractional retinal detachment (data not shown). Furthermore, any damage of the lens caused cataract formation (3%–5% incidence rate), which was observed several days after the injection. Animals with such complications were excluded from analysis.

Tissue Preparation for Histology

Mice were anesthetized with 50 mg/kg pentobarbital (Nembutal; Abbott Laboratories, Santa Clara, CA) and eyes were fixed by transcardiac perfusion with formaldehyde and glutaraldehyde (1% and 2%, respectively) in 0.1 M sodium phosphate buffer (pH 7.4). After the eyes were enucleated, the posterior portion of each eye, containing the retina and retinal pigment epithelium was fixed additionally for 24 hours in 0.1 M phosphate buffer (pH 7.4) containing 2% formaldehyde and 2.5% glutaraldehyde. The tissues were then osmicated, dehydrated through a graded ethanol series, embedded in paraffin, and processed for histologic sectioning. The sections (0.5 μm thick) were cut along the horizontal meridian, passed through the optic nerve, and stained with hematoxylin and eosin (H&E) in preparation for light microscopy. For each time point, three to six animals were used to evaluate retinal histology. The extent of retinal detachment was determined by drawing a measurement arc covering the region of physical separation of neural retina from RPE. The lengths of these arcs were calculated using computer-based interactive measurements (Axiovision; Carl Zeiss Meditec, Oberkochen, Germany).

For the evaluation of fluorescent microbead distribution, mice were anesthetized as described earlier and fixed by transcardiac perfusion with 4% paraformaldehyde for cryostat sectioning. After enucleation and a 1-hour fixation in 4% paraformaldehyde, the anterior segments were removed, and eyes were fixed overnight at 4°C. The following day, eyecups were washed in PBS and transferred to a 30% sucrose solution for cryoprotection. After embedding in mounting matrix (M-1; Shandon, Pittsburgh, PA), 5 μm sections were cut approximately along the horizontal meridian, passing through the optic nerve. For statistical evaluation, three to six eyes were evaluated for the distribution of fluorescent microbeads after subretinal delivery.

Electroretinogram and Statistical Analysis

After at least 4 hours of dark adaptation, animals were anesthetized (as indicated in the injection protocol), vibrissae were trimmed, and the eyes were dilated using 2.5% phenylephrine. Animals were placed on a regulated heating pad throughout the experiment. Electroretinograms (ERGs) were recorded using a stainless steel wire contacting the corneal surface through a layer of 2.5% methylcellulose. Needle elec-

trodes in the cheek and tail of the animal served as reference and ground leads, respectively. Responses were differentially amplified (half bandpass, 1–4000 Hz), averaged, and stored by using a signal-averaging system (Compact 4; Nicolet, Madison, WI). For the assessment of rod photoreceptor function, a strobe flash stimulus was presented to the dark-adapted, dilated eyes in a Ganzfeld (model GS-2000; Nicolet) with a 137-cd (sec/m^2) flash intensity. The amplitude of the a-wave was measured from the prestimulus baseline to the a-wave trough. The amplitude of the b-wave was measured from the trough of the a-wave to the crest of the b-wave. To evaluate the recovery of cone photoreceptors in *rds*$^{+}$/$^{-}$ mice, animals were light adapted for 5 minutes under a light source of 29.02 cd/m^2 intensity. After this period of light-adaptation, a strobe flash stimulus was presented to the dilated eyes in the Ganzfeld with a 77-cd (sec/m^2) flash intensity. The amplitude of the cone b-wave was measured from the trough of the a-wave to the crest of the b-wave.

One-way analysis of variance (ANOVA) and post-hoc tests using Bonferroni's pair-wise comparisons were used to determine the significance of differences in the ERG amplitudes after subretinal injection with the different treatments (Prism, ver. 3.02; GraphPad, San Diego, CA).

TUNEL Detection after Subretinal Injection

Animals were subretinally injected with either 1 μL of saline, INS37217 (10 μM), or mock-injected and killed 48 hours PI. After death and enucleation, the anterior segments of eyes were removed and the posterior portion placed in 4% paraformaldehyde overnight. In preparation for cryostat sectioning, eyes were placed in a 30% solution of sucrose overnight, embedded in M-1 matrix (Shandon), and sectioned throughout the entire eyecup at a 10-μm thickness. TUNEL detection was performed according to manufacturer guidelines for cell death detection (In Situ Cell Death Detection Kit, TMR red; Roche Applied Sciences, Mannheim, Germany). After completing the labeling and washing, slides were coverslipped using antifade mounting medium for fluorescence (Vector Laboratories, Burlingame, CA).

Results

Time Course of Retinal Reattachment

Histologic cross sections spanning the meridian of the eye were used to evaluate the extent and time course of retinal detachment and reattachment at 0 to 1 hour, 8 hours, and 1, 3, and 7 days after a single 1-μL subretinal injection of saline (Fig. 1). Retinal detachment was defined as a morphologically evident, physical separation of neural retina from RPE. This separation appeared greatest near the site of injection, and tapered in effect at sections distal from the site of injection. Representative sections are shown in Figures 1A–F. The gross morphologic extent of retinal detachment (measured in millimeters) was assessed throughout the cross section of the eye that contained the site of injection. As shown in Figure 1G, the values were averaged and plotted for each time point. At 0 to 1 hour PI, approximately 60% of the retina was detached (Fig. 1B). By 8 hours PI, there was an extensive decrease in the level of retinal detachment (Fig. 1C), and gross reattachment appeared complete by 24 hours PI (Fig. 1D). However, extensive retinal folding was also observed at 1 day PI (Fig. 1D) and as late as 3 days PI (Fig. 1E). This retinal folding appeared fully resolved at 7 days PI (Fig. 1F). We observed faint remnants of retinal restructuring at 7 days PI in some eyes (Fig. 1F; boxed area), but in most of the animals, the retinal folding appeared completely resolved at the site of injection (data not shown).

Distribution of the Injected Material in the Subretinal Space

To examine the distribution of the injected material in the subretinal space, animals were subretinally injected with 1 μL saline containing fluorescent microbeads and then examined either immediately after the injection (0–1 hour) or 7 days PI. The distribution of the microbeads was assessed by fluorescence microscopy (Figs. 2, 3). Immediately after the injection, nonuniform retinal blebs were apparent throughout the eyecup as an indicator of retinal detachment caused by the injection (Fig. 2A). The fluorescent microbeads were distributed throughout the eyecup. Figure 2B shows a representative cross section of the eyecup taken 1 hour after the injection and centered around the site of injection. Higher magnification of Nomarski and fluorescence overlay (Figs. 2C–F) and their corresponding fluorescence images alone (Figs. 2G–J) of the areas indicated by rectangles in Figure 2B clearly reflect the level of retinal detachment and the distribution of fluorescent beads in the subretinal space. Although the beads were distributed throughout the retina, a higher concentration was observed at the site of injection (Figs. 2I, 2J), gradually decreasing in sections away from the injection site (Figs. 2G, 2H).

After retinal reattachment, Figure 3A shows a flattened eyecup 7 days PI, demonstrating the distribution of beads throughout the entire eye. A cross section of these eyes showed most of the beads to be located in the RPE (Fig. 3B). To confirm fluorescent microbead distribution, we removed the retina and washed the eyecup three times with saline to eliminate any remnants of beads in the subretinal space. Although some beads were detected in the washes, most of them were retained in the RPE (Fig. 3C). The washed eyecup was then cryosectioned and analyzed histologically (Fig. 3D). Fluorescence images of these sections show the localization of the fluorescent microbeads inside the RPE cells (Fig. 3E), indicating the regained ability of RPE cells to phagocytose materials immediately after retinal reattachment.

Recovery of the Dark-Adapted Rod Responses after Retinal Reattachment

Dark-adapted ERG recordings were conducted at 1, 3, 7, 14, and 60 days after injection of 1 μL saline in normal mice. Both dark-adapted a- and b-wave amplitudes showed an improvement in rod function over the 60-day recording period (Fig. 4). At 1 day PI, dark-adapted a- and b-wave amplitudes were reduced approximately 60% compared with those of mock-injected animals ($P < 0.001$; Bonferroni's pair-wise test). The recovery of dark-adapted ERG amplitudes continued with the progression of time. However, the data demonstrate that even at day 14 after retinal detachment, both rod a- and b-wave amplitudes remained significantly less than in mock-injected control eyes. Finally, at 60 days PI, the retina produced a dark-adapted ERG response that was comparable to that in mock-injected eyes.

Effect of INS37217 on Rod Functional Recovery after Retinal Detachment in Normal Mice

Dark-adapted ERG recordings were made from normal mice at 1 and 10 days after a 1-μL subretinal injection of saline alone or of saline containing INS37217 at concentrations ranging from 1 to 200 μM. Figure 5A shows the dose–response curve at day 1 PI. Select doses of INS37217 produced a significant increase in dark-adapted a- and b-wave amplitudes when compared with saline-injected eyes. The effects of INS37217 appear to follow a "bell-shaped" dose–response curve. Of the doses used in this study, one-way ANOVA and Bonferroni's pair-wise comparison revealed a statistically significant ($P < 0.05$) improvement in a-wave ERG recovery with the 10-μM dose (Fig. 5A, asterisks). In terms of b-wave recovery, eyes injected with 10 and 20 μM of INS37217 showed a statistically significant ($P < 0.05$) improvement when compared with saline-injected eyes (Fig. 5A, asterisks). Rod ERG function continued to recover in this pattern, showing a more significant ($P < 0.001$) recovery in

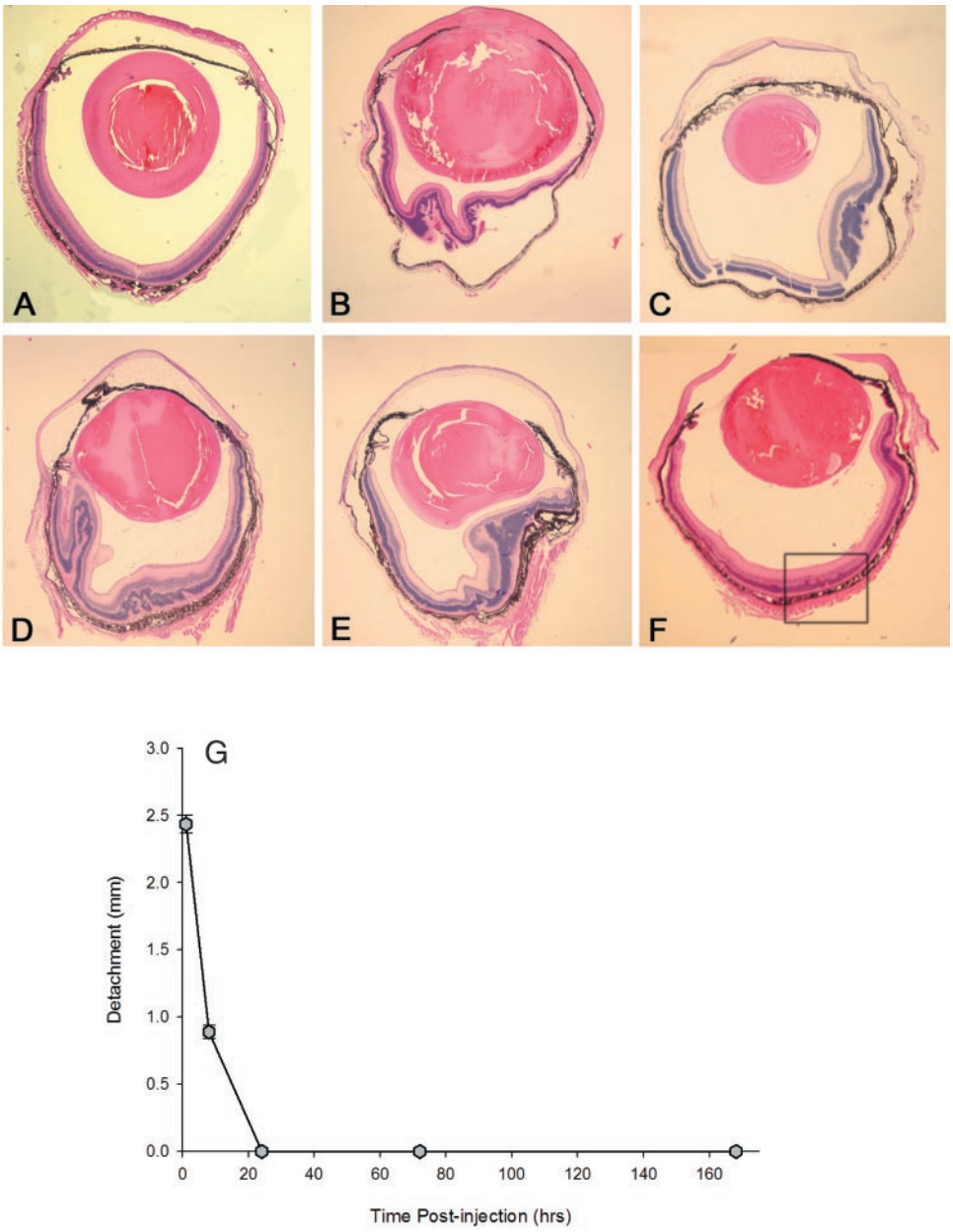

FIGURE 1. Recovery of retinal morphology after retinal detachment. The entire eye globe was sectioned and only H&E-stained sections at the site of injection are presented to show the extent of retinal detachment at the site of injection in a control eye (**A**) and in eyes injected subretinally with 1 μL saline and evaluated at 0 to 1 hour (**B**), 8 hours (**C**), and 1 (**D**), 3 (**E**), and 7 (**F**) days PI. Retinal detachment was defined as the physical separation of the neural retina from the RPE. The extent of retinal detachment was determined by drawing a measurement arc covering the region of physical separation of neural retina from RPE. The lengths of these arcs were calculated by using computer-based interactive measurements. (**G**) Averaged and quantified areas of retinal detachment at various time points PI (0–1 hour, 1 day [24 hours], 3 days [72 hours], and 7 days [168 hours]). The retina achieved reattachment to the RPE as early as 1 day after subretinal delivery. Morphologically, the retina returned to an unfolded, attached state 7 days PI. For statistical evaluation, three to six eyes were evaluated for the distribution of fluorescent microbeads after subretinal delivery.

INS37217- versus saline-injected eyes up to 10 days PI (Figs. 5B, 5C, asterisks). At 10 days after retinal detachment, INS37217-treated eyes showed an approximate 90% recovery of rod ERG function when compared to the 50% recovery in the saline-injected eyes. Figure 5B shows representatives of dark-adapted ERG waveforms taken from mock-, saline-, and INS37217-injected eyes at 10 days PI. Averages of these treatment groups are shown in Figure 5C, further demonstrating the favorable effects of this compound.

Effect of INS37217 on Functional Recovery after Retinal Reattachment in an *rds*$^{+/-}$ Mouse Model of Retinitis Pigmentosa

The effects of subretinal injection of saline (1 μL) with or without INS37217 (10 μM) on dark- and light-adapted ERG responses were also evaluated in 1-month-old *rds*$^{+/-}$ mice and compared with mock-injected eyes. The functional recovery was monitored 1 day after subretinal injection. Although the rate of retinal degeneration is slow in *rds*$^{+/-}$ mice, the abnormality in photoreceptor outer segment structure results in an approximate 65% reduction in rod ERG response by 1 month of age, whereas cone-specific ERG responses remain unaffected at this age.[40] In INS37217-treated eyes, significant increases in dark-adapted a- and b-wave amplitudes (Figs. 6A, 6B) and in light-adapted cone b-wave amplitudes (Figs. 6C, 6D) were observed when compared with saline-injected control eyes ($P < 0.05$). Representative ERG waveforms in Figures 6A and 6C illustrate this enhancement in ERG function afforded by the 10-μM dose of INS37217 under dark- and light-adapted conditions, respectively. This finding demonstrates the ability of INS37217 to have a positive effect on the enhancement of functional recovery of rods and cones, even in a degenerating mouse retina.

Effect of INS37217 on Retinal Folding and the Number of TUNEL-Positive Cells after Retinal Reattachment in Normal Mice

In saline-injected eyes, most retinal folding occurred at the site of injection (Figs. 1, 2). Figure 7 demonstrates the extent of

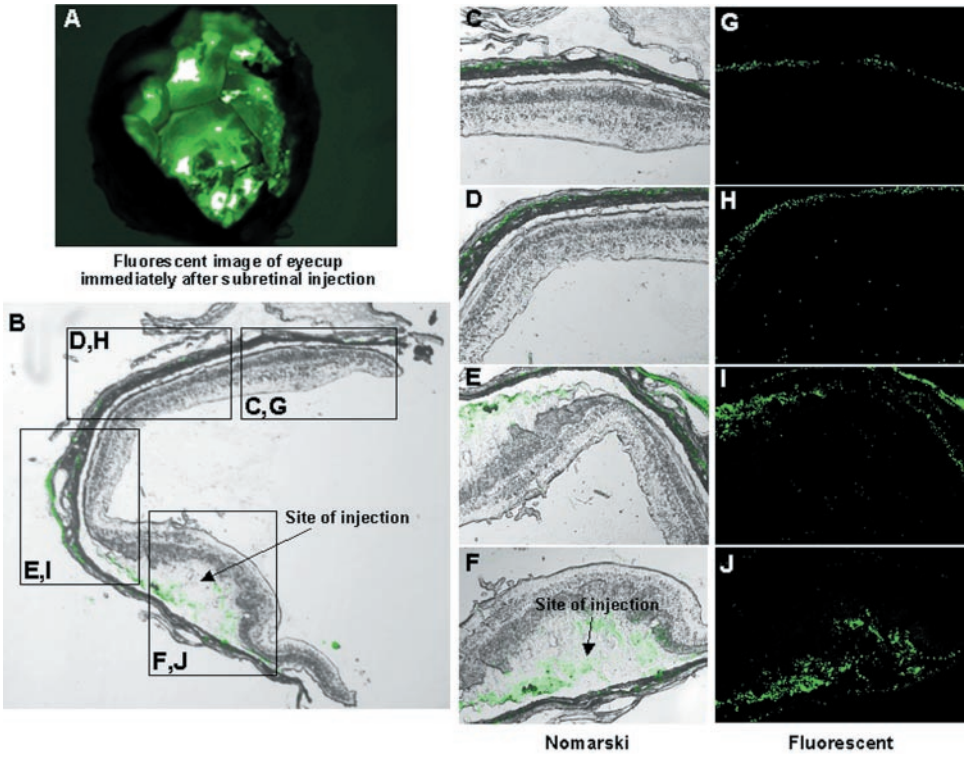

FIGURE 2. Distribution of the injected material in the subretinal space of the mouse eye at 0 to 1 hour PI. (**A**) A representative fluorescence image of an eyecup (without the anterior segment) showing retinal blebs and the distribution of the fluorescent microbeads to most of the eye. (**B**) Cross section of an eye showing the structure of the retina at the site of injection and the distribution of the fluorescent microbeads to almost all of the subretinal space. Areas highlighted with *rectangles* were examined at higher magnifications and represent a composite overlay of Nomarski and fluorescence (**C–F**) and their corresponding images under fluorescence microscopy alone (**G–J**). *Arrows* in (**B**) and (**F**): detachment at the site of injection.

retinal folding in saline-injected and INS37217-injected (10 μM) eyes 2 days PI after complete morphologic reattachment had occurred. When compared with saline-injected eyes (Figs. 7C, 7E), INS37217-treated retinas achieved morphologic reattachment with dramatically less folding, even at the site of injection (Figs. 7D, 7F, needle track in D). Representative sections also show a correlation between photoreceptors residing in the folded region of the retina and TUNEL-positive staining (Figs. 7C–F). After examination of cross sections spanning the entire eyecup of injected mice, evaluation showed a dramatic reduction in the number of TUNEL-positive cells in INS37217 (10 μM)-treated eyes (Figs. 7D, 7F) when compared with their saline-injected counterparts (Figs. 7C, 7E). Mock-injected animals showed neither retinal folding (Fig. 7A) nor TUNEL-positive photoreceptor cells throughout the entire eyecup (Fig. 7B).

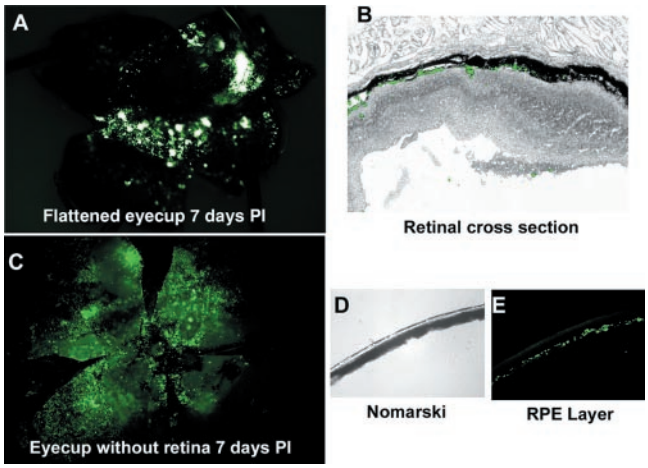

FIGURE 3. The distribution of fluorescent microbeads in injected mouse eye 7 days PI. (**A**) Fluorescence image of a representative flattened eyecup revealed retinal reattachment and the spread of the injected material throughout the entire eye. (**B**) Retinal cross section that represents a composite overlay of Nomarski and fluorescence image shows the structure of the retina at the site of injection and the distribution of the fluorescent microbeads to most of the subretinal space. (**C**) A representative fluorescence image of a flattened eyecup without the retina showing the distribution of the beads in the RPE layer. After the retina was removed, the eyecup was washed with PBS to remove remnants of the beads in the subretinal space. The fluorescent microbeads appear to have been phagocytosed by RPE cells. (**D**) Cross section of the eyecup in (**C**), to confirm the localization of the fluorescent microbeads to the RPE. (**E**) A corresponding fluorescence image of the RPE layer shown in (**D**).

DISCUSSION

With the most recent developments in prospective gene therapies for retinal diseases[26,43–48] and their great promise for clinical applications,[28] it is critical to measure the efficacy of these therapies in well-characterized animal models with phenotypes closely resembling those of patients. The mouse eye is widely used as a model for a variety of human ocular diseases and can therefore be used to test the efficacy of novel therapeutic approaches for treating human retinal diseases. So far, the most effective means of delivering gene therapies to the photoreceptor and RPE cells is through subretinal delivery. However, any volume injected in the subretinal space causes a temporary retinal detachment. Persistence of this detachment leads to many negative consequences that impact visual function. Because the interaction between photoreceptors and RPE is vital, one must balance the resultant detachment needed for the distribution of therapeutic agent with that of the pathologic state caused by the detachment.[1,2,33,49] Although in the normal retina, retinal reattachment after temporary detachment eventually leads to a relatively complete recovery of morphology and function,[4,42,50] cell death still occurs.[1] No study to date has shown the effect of experimental retinal detachment on the recovery of either retinal morphology or visual function in animal models of retinal degeneration.

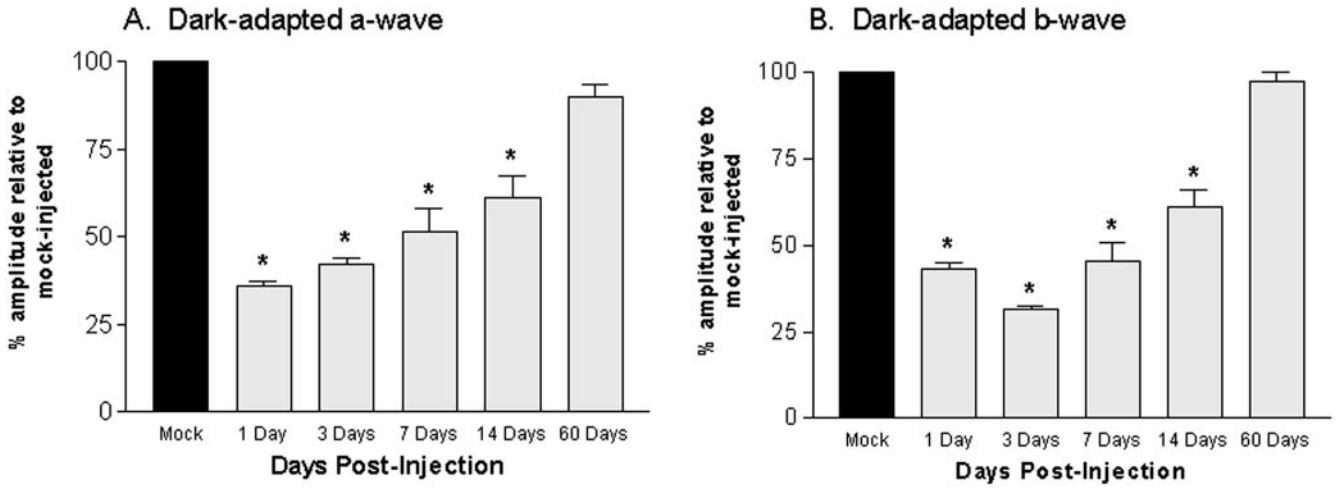

FIGURE 4. Time course of dark-adapted ERG recovery in the normal mouse eye after retinal reattachment. (**A**) Dark-adapted a- and (**B**) b-wave amplitudes recorded at 1, 3, 7, 14, and 60 days PI of 1 μL of saline. Both a- and b-wave amplitudes show an improvement in function over time. The gradual recovery in rod ERG function reached a normal level by 60 days. Control mock-injected values represent results from the contralateral eye of saline-injected animals. These eyes underwent corneal puncture without injection. ERG values represent averages of 8 to 12 eyes per treatment.

In the current study, a single subretinal injection of 1 μL saline solution containing fluorescent microbeads caused a retinal detachment and distributed the microbeads to almost all of the subretinal space. Gross histologic evaluation revealed that spontaneous retinal reattachment occurred within 24 hours PI and retinal folding was observed for another 2 days but appeared largely resolved by 7 days after the initial detachment. Functional recovery, as determined by ERG responses, did not correlate with the rate of morphologic reattachment. In mice, the recovery of dark-adapted a-wave ERG amplitudes at 1, 3, 7, 14, and 60 days after a single subretinal injection was shown to be, respectively, 36%, 42%, 52%, 61%, and 90% of the a-wave of mock-injected control mice (100%). The recovery of dark-adapted b-wave ERG amplitudes for the same time points were 44%, 31%, 45%, 61%, and 98% of the b-wave of mock-injected control animals. This dissociation between time course of morphologic reattachment and functional recovery, in part, reflects retinal restructuring that occurs as a result of retinal detachment and persists even after achieving a significant level of reattachment.[1,15,51] These results are consistent with clinical findings that report that full visual recovery lags behind successful surgical reattachment[14] and are further supported by studies in the rabbit and the squirrel.[15,52] Our present findings, along with previous reports of compromised retinal function after retinal reattachment in humans and in experimental animal models, prompted us to evaluate the use of a pharmacological approach for enhancing recovery of retinal ERG function after detachment in mice.

Earlier studies have demonstrated that the synthetic $P2Y_2$ receptor agonist INS37217 stimulates subretinal fluid reabsorption and improves the rates of retinal reattachment in rat and rabbit models of experimental retinal detachment.[38,39] Herein, we show that subretinal injection of saline solution containing INS37217 (10 μM) significantly enhanced recovery of a- and b-wave amplitudes at 1 and 10 days PI in normal mice, when compared with saline-injected control animals. Of the doses of INS37217 tested, the ERG rescue effect of 10 μM INS37217 appeared optimal. The reason for the absence of protective effect on ERG function at higher INS37217 concentrations is unknown and remains to be investigated. However, we observed no obvious toxicological effect of INS37217 on the retina at higher concentrations, a finding that is consistent with previous rabbit ERG studies of intravitreally administered INS37217.[38] We also report that, when compared with saline-injected controls, INS37217 (10 μM) also enhanced the recovery of rod and cone functions in 1-month old $rds^{+/-}$ mice. This enhancement in functional recovery persisted at 10 days PI (data not shown). The data in the $rds^{+/-}$ mouse model of retinitis pigmentosa demonstrate a protective effect of INS37217 on rod and cone function after experimental detachment in a relatively advanced stage of photoreceptor dysfunction. This finding has direct implications for the potential use of subretinal injection as a means of delivering therapeutic agents in patients.

Although studies have shown that factors such as brain-derived neurotrophic factor (BDNF) and glial-derived neurotrophic factor (GDNF)[53,54] (Lewis GP, et al. *IOVS* 1998;39:ARVO Abstract 2647), as well as oxygen supplementation[55–57] reduces photoreceptor cell death and mitigates the progression of a number of detachment-induced retinopathic changes in experimental animals, the effects of these factors on functional recovery after retinal reattachment have not been reported. Our present findings with INS37217 represent the first example of the use of a pharmacological agent to improve ERG

FIGURE 5. Dose–response curve of the effect of INS37217 on the functional recovery of the dark-adapted ERG after retinal detachment in normal mice. (**A**) The effects of INS37217 at concentrations ranging from 1 to 200 μM on the recovery of the dark-adapted a- and b-wave amplitudes at 1 day PI. The 10-μM dose of INS37217 elicited the most significant recovery in dark-adapted rod function when compared with saline injected eyes. (**B**) Representative dark-adapted ERG waveforms from mock-injected, saline, and INS37217-injected eyes recorded at 10 days PI demonstrating the long-term ability of INS37217 to enhance significantly the recovery of rod-ERG function after retinal detachment. (**C**) The pattern of ERG recovery in both a- and b-wave amplitudes resulting from the 10-μM dose of INS37217 persisted until 10 days PI. At this time point, the saline injected eyes recovered approximately 50% of the rod ERG, whereas the INS37217-injected eyes recovered 90% of the rod-ERG. ERGs were also obtained from saline injected contralateral eyes. *Statistically significant difference between INS37127- and saline-injected eyes. ERG values represent averages of 8 to 12 eyes per treatment.

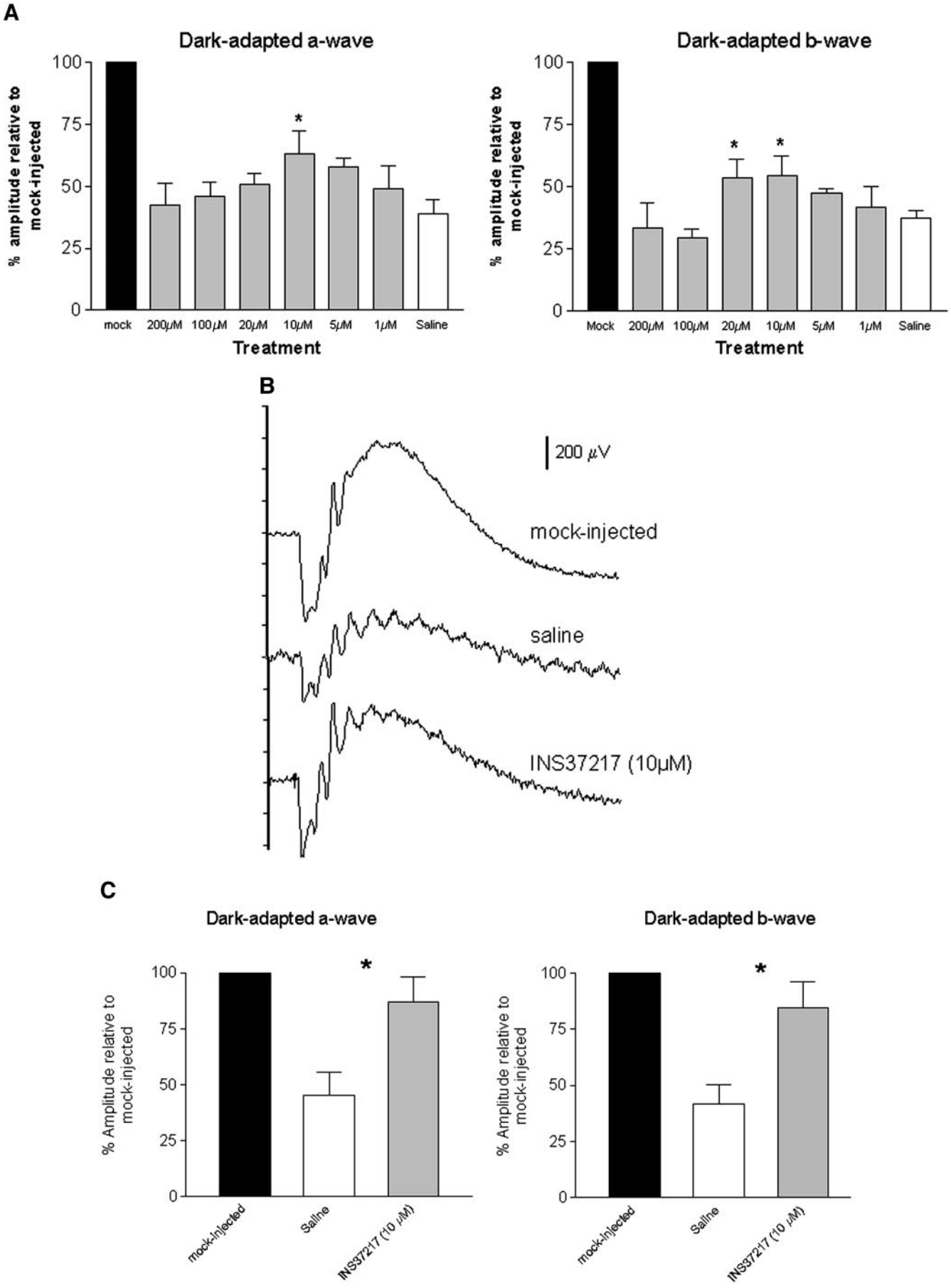

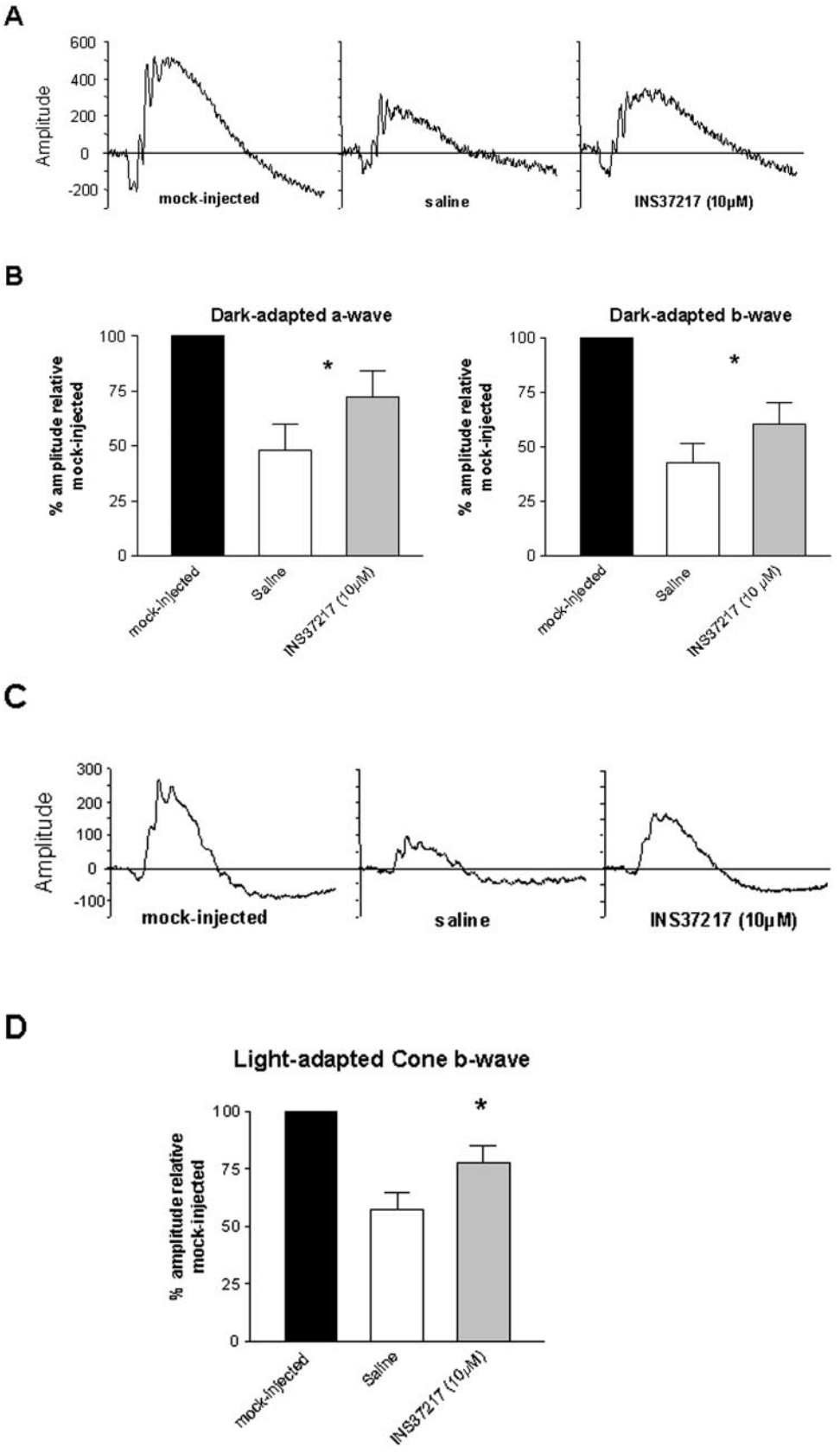

FIGURE 6. Effect of INS37217 on the recovery of the dark- and light-adapted ERG after retinal reattachment in the $rds^{+/-}$ mice. (**A**) Representatives of the dark-adapted ERG waveforms from saline-, INS37217-, and mock-injected eyes at 1 day PI reflect the enhancement in the rod function afforded by the 10-μM dose of INS37217. (**B**) Dark-adapted ERG a- and b-wave amplitudes recorded at 1-day PI from animals that were mock-injected control, saline-injected, or saline+INS37217 (10 μM)-injected animals. Data are averaged from 8 to 10 independent measurements. (**C**) Representative light-adapted waveforms showing the enhanced recovery of the cone ERG amplitudes as a result of injection of INS37217. (**D**) The average values of the recovery of the light-adapted b-wave from eight independent measurements showing a significant enhancement in cone function afforded by the 10-μM dose of INS37217. Data were also obtained from saline injections in the contralateral eye of the INS37217-injected animals. ERG values represent averages of 8 to 12 eyes per treatment.

function after experimental retinal reattachment in healthy eyes and in a model of inherited photoreceptor degeneration. Although the underlying mechanism driving this ERG-enhancing effect of INS37217 in mice needs further examination, notable differences in retinal morphology were detected between saline and INS37217-injected eyes as early as 2 days after

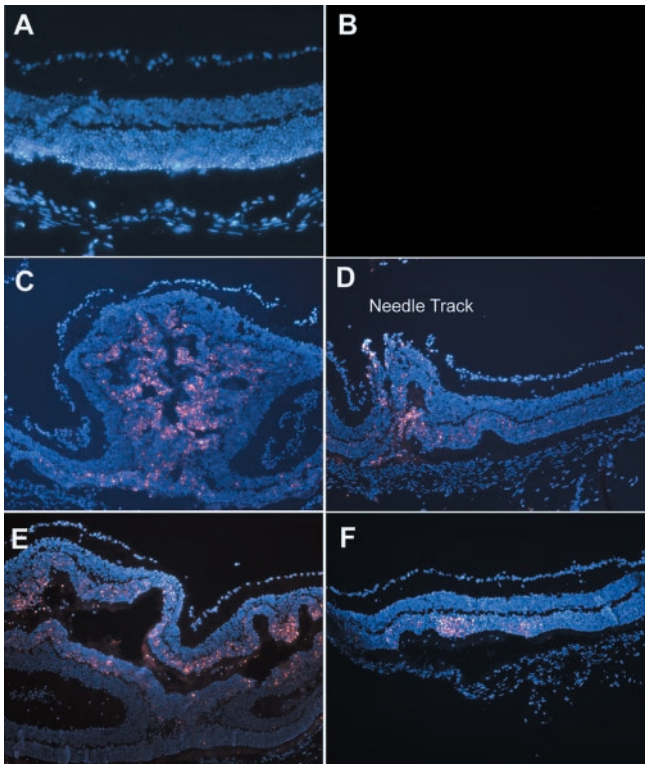

FIGURE 7. Detection of TUNEL-positive cells in saline- versus INS37217-injected retinas. (**A**) Representative fluorescence image of a retinal cross section at 2 days PI shows a mock-injected eye stained with DAPI without any retinal detachment. (**B**) TUNEL staining of the same section showing the absence of TUNEL-positive photoreceptors. (**C**, **E**) Representative fluorescence images of retinal cross sections 2 days after saline injection, taken from two unrelated representative eyes stained with DAPI (*blue*) and TUNEL (*red*). Both sections were obtained at the site of injection and show a significant level of retinal detachment and a high number of TUNEL-positive photoreceptor cells. (**D**, **F**) Retinal cross section from two independent samples at the same time point injected with INS37217 and stained with DAPI (*blue*) and TUNEL (*red*). Both sections show significant reduction in the level of retinal detachment and number of TUNEL-positive photoreceptor cells. Indicated in (**D**) is an example of the needle track at the site of injection.

retinal detachment. Significantly fewer retinal folds were seen at the site of injection in INS37217 (10 μM)-treated eyes compared with their saline-injected counterparts. More significantly, the number of TUNEL-positive photoreceptor cells was reduced in the presence of INS37217. Because TUNEL staining has been widely accepted as an indicator of cell death, it is reasonable to suggest that INS37217 reduces photoreceptor cell death by stimulating more efficient retinal reattachment, therefore improving the intimate interactions between photoreceptor outer segments and the RPE.

In summary, we describe the enhanced recovery of retinal morphology and function after the administration of INS37217. This recovery is probably due to reduced morphologic rearrangements and cell death associated with retinal detachment. When taken together, these findings support the future use of this $P2Y_2$ receptor agonist in the clinical resolution of retinal detachment and in enhancement of functional recovery after subretinally delivered therapies.

Acknowledgments

The authors thank Adrian Timmers for demonstrating transvitreal subretinal injection and Rusty Montgomery and Kathy Alvarez for technical assistance.

References

1. Cook B, Lewis GP, Fisher SK, et al. Apoptotic photoreceptor degeneration in experimental retinal detachment. *Invest Ophthalmol Vis Sci*. 1995;36:990–996.
2. Fisher SK, Erickson PA, Lewis GP, et al. Intraretinal proliferation induced by retinal detachment. *Invest Ophthalmol Vis Sci*. 1991; 32:1739–1748.
3. Lewis GP, Guerin CJ, Anderson DH, et al. Rapid changes in the expression of glial cell proteins caused by experimental retinal detachment. *Am J Ophthalmol*. 1994;118:368–376.
4. Lewis GP, Charteris DG, Sethi CS, et al. Animal models of retinal detachment and reattachment: identifying cellular events that may affect visual recovery. *Eye*. 2002;16:375–387.
5. Lewis GP, Fisher SK. Muller cell outgrowth after retinal detachment: association with cone photoreceptors. *Invest Ophthalmol Vis Sci*. 2000;41:1542–1545.
6. Lewis GP, Linberg KA, Fisher SK. Neurite outgrowth from bipolar and horizontal cells after experimental retinal detachment. *Invest Ophthalmol Vis Sci*. 1998;39:424–434.
7. Rex TS, Fariss RN, Lewis GP, et al. A survey of molecular expression by photoreceptors after experimental retinal detachment. *Invest Ophthalmol Vis Sci*. 2002;43:1234–1247.
8. Young RW, Bok D. Participation of the retinal pigment epithelium in the rod outer segment renewal process. *J Cell Biol*. 1969;42: 392–403.
9. Bridges CD. Vitamin A and the role of the pigment epithelium during bleaching and regeneration of rhodopsin in the frog eye. *Exp Eye Res*. 1976;22:435–455.
10. Liou GI, Bridges CD, Fong SL, et al. Vitamin A transport between retina and pigment epithelium–an interstitial protein carrying endogenous retinol (interstitial retinol-binding protein). *Vision Res*. 1982;22:1457–1467.
11. Bernstein PS, Law WC, Rando RR. Isomerization of all-trans-retinoids to 11-cis-retinoids in vitro. *Proc Natl Acad Sci USA*. 1987;84: 1849–1853.
12. Li JD, Gallemore RP, Dmitriev A, et al. Light-dependent hydration of the space surrounding photoreceptors in chick retina. *Invest Ophthalmol Vis Sci*. 1994;35:2700–2711.
13. Dmitriev AV, Govardovskii VI, Schwahn HN, et al. Light-induced changes of extracellular ions and volume in the isolated chick retina-pigment epithelium preparation. *Vis Neurosci*. 1999;16: 1157–1167.
14. Burton TC. Recovery of visual acuity after retinal detachment involving the macula. *Trans Am Ophthalmol Soc*. 1982;80:475–497.
15. Sakai T, Calderone JB, Lewis GP, et al. Cone photoreceptor recovery after experimental detachment and reattachment: an immunocytochemical, morphological, and electrophysiological study. *Invest Ophthalmol Vis Sci*. 2003;44:416–425.
16. Liem AT, Keunen JE, van Meel GJ, et al. Serial foveal densitometry and visual function after retinal detachment surgery with macular involvement. *Ophthalmology*. 1994;101:1945–1952.
17. Kusaka S, Toshino A, Ohashi Y, et al. Long-term visual recovery after scleral buckling for macula-off retinal detachments. *Jpn J Ophthalmol*. 1998;42:218–222.
18. Berson EL. Retinitis pigmentosa: unfolding its mystery. *Proc Natl Acad Sci USA*. 1996;93:4526–4528.
19. Li T, Sandberg MA, Pawlyk BS, et al. Effect of vitamin A supplementation on rhodopsin mutants threonine-17→methionine and proline-347→serine in transgenic mice and in cell cultures. *Proc Natl Acad Sci USA*. 1998;95:11933–11938.
20. Frasson M, Sahel JA, Fabre M, et al. Retinitis pigmentosa: rod photoreceptor rescue by a calcium-channel blocker in the rd mouse. *Nat Med*. 1999;5:1183–1187.
21. Bok D, Yasumura D, Matthes MT, et al. Effects of adeno-associated virus-vectored ciliary neurotrophic factor on retinal structure and function in mice with a P216L rds/peripherin mutation. *Exp Eye Res*. 2002;74:719–735.
22. LaVail MM, Yasumura D, Matthes MT, et al. Protection of mouse photoreceptors by survival factors in retinal degenerations. *Invest Ophthalmol Vis Sci*. 1998;39:592–602.

23. Cayouette M, Behn D, Sendtner M, et al. Intraocular gene transfer of ciliary neurotrophic factor prevents death and increases responsiveness of rod photoreceptors in the retinal degeneration slow mouse. *J Neurosci*. 1998;18:9282–9293.
24. Cayouette M, Smith SB, Becerra SP, et al. Pigment epithelium-derived factor delays the death of photoreceptors in mouse models of inherited retinal degenerations. *Neurobiol Dis*. 1999;6:523–532.
25. Takahashi M, Miyoshi H, Verma IM, et al. Rescue from photoreceptor degeneration in the rd mouse by human immunodeficiency virus vector-mediated gene transfer. *J Virol*. 1999;73:7812–7816.
26. Bennett J, Zeng Y, Bajwa R, et al. Adenovirus-mediated delivery of rhodopsin-promoted bcl-2 results in a delay in photoreceptor cell death in the rd/rd mouse. *Gene Ther*. 1998;5:1156–1164.
27. Lewin AS, Drenser KA, Hauswirth WW, et al. Ribozyme rescue of photoreceptor cells in a transgenic rat model of autosomal dominant retinitis pigmentosa. *Nat Med*. 1998;4:967–971.
28. Acland GM, Aguirre GD, Ray J, et al. Gene therapy restores vision in a canine model of childhood blindness. *Nat Genet*. 2001;28:92–95.
29. Bennett J, Tanabe T, Sun D, et al. Photoreceptor cell rescue in retinal degeneration (rd) mice by in vivo gene therapy. *Nat Med*. 1996;2:649–654.
30. Liang FQ, Aleman TS, Dejneka NS, et al. Long-term protection of retinal structure but not function using RAAV: CNTF in animal models of retinitis pigmentosa. *Mol Ther*. 2001;4:461–472.
31. LaVail MM, Yasumura D, Matthes MT, et al. Ribozyme rescue of photoreceptor cells in P23H transgenic rats: long-term survival and late-stage therapy. *Proc Natl Acad Sci USA*. 2000;97:11488–11493.
32. Takeuchi A, Kricorian G, Yao XY, et al. The rate and source of albumin entry into saline-filled experimental retinal detachments. *Invest Ophthalmol Vis Sci*. 1994;35:3792–3798.
33. Lewis GP, Matsumoto B, Fisher SK. Changes in the organization and expression of cytoskeletal proteins during retinal degeneration induced by retinal detachment. *Invest Ophthalmol Vis Sci*. 1995;36:2404–2416.
34. Machemer R. Macular translocation. *Am J Ophthalmol*. 1998;125:698–700.
35. Pederson JE, MacLellan HM. Experimental retinal detachment. I. Effect of subretinal fluid composition on reabsorption rate and intraocular pressure. *Arch Ophthalmol.* 1982;100:1150–1154.
36. Peterson WM, Meggyesy C, Yu KF, et al. Extracellular ATP activates calcium signaling, ion, and fluid transport in retinal pigment epithelium. *J Neurosci*. 1997;17:2324–2337.
37. Ryan JS, Baldridge WH, Kelly MEM. Purinergic regulation of cation conductances and intracellular Ca2+ in cultured rat retinal pigment epithelial cells. *J Physiol* (*Lond*) 1999;520:745–759.
38. Meyer CH, Hotta K, Peterson WM, et al. Effect of INS37217, a P2Y(2) Receptor Agonist, on Experimental Retinal Detachment and Electroretinogram in Adult Rabbits. *Invest Ophthalmol Vis Sci*. 2002;43:3567–3574.
39. Maminishkis A, Jalickee S, Blaug SA, et al. The P2Y(2) receptor agonist INS37217 stimulates RPE fluid transport in vitro and retinal reattachment in rat. *Invest Ophthalmol Vis Sci*. 2002;43:3555–3566.
40. Cheng T, Peachey NS, Li S, et al. The effect of peripherin/rds haploinsufficiency on rod and cone photoreceptors. *J Neurosci*. 1997;17:8118–8128.
41. Travis GH, Brennan MB, Danielson PE, et al. Identification of a photoreceptor-specific mRNA encoded by the gene responsible for retinal degeneration slow (rds). *Nature*. 1989;338:70–73.
42. Timmers AM, Zhang H, Squitieri A, et al. Subretinal injections in rodent eyes: effects on electrophysiology and histology of rat retina. *Mol Vis*. 2001;7:131–137.
43. Flannery JG, Zolotukhin S, Vaquero MI, et al. Efficient photoreceptor-targeted gene expression in vivo by recombinant adeno-associated virus. *Proc Natl Acad Sci USA*. 1997;94:6916–6921.
44. Hauswirth WW, LaVail MM, Flannery JG, et al. Ribozyme gene therapy for autosomal dominant retinal disease. *Clin Chem Lab Med*. 2000;38:147–153.
45. Miyoshi H, Takahashi M, Gage FH, et al. Stable and efficient gene transfer into the retina using an HIV-based lentiviral vector. *Proc Natl Acad Sci USA*. 1997;94:10319–10323.
46. Bennett J, Duan D, Engelhardt JF, et al. Real-time, noninvasive in vivo assessment of adeno-associated virus-mediated retinal transduction. *Invest Ophthalmol Vis Sci*. 1997;38:2857–2863.
47. Ali RR, Reichel MB, De Alwis M, et al. Adeno-associated virus gene transfer to mouse retina. *Hum Gene Ther*. 1998;9:81–86.
48. Zeng Y, Rosborough RC, Li Y, et al. Temporal and spatial regulation of gene expression mediated by the promoter for the human tissue inhibitor of metalloproteinases-3 (TIMP-3)-encoding gene. *Dev Dyn*. 1998;211:228–237.
49. Geller SF, Lewis GP, Anderson DH, et al. Use of the MIB-1 antibody for detecting proliferating cells in the retina. *Invest Ophthalmol Vis Sci*. 1995;36:737–744.
50. Lewis GP, Charteris DG, Sethi CS, et al. The ability of rapid retinal reattachment to stop or reverse the cellular and molecular events initiated by detachment. *Invest Ophthalmol Vis Sci*. 2002;43:2412–2420.
51. Hisatomi T, Sakamoto T, Goto Y, et al. Critical role of photoreceptor apoptosis in functional damage after retinal detachment. *Curr Eye Res*. 2002;24:161–172.
52. Kim SD, Nao-i N, Maruiwa F, et al. Electrical responses from locally detached retina and its recovery after reattachment. *Ophthalmologica*. 1996;210:195–199.
53. Wu WC, Lai CC, Chen SL, et al. Gene therapy for detached retina by adeno-associated virus vector expressing glial cell line-derived neurotrophic factor. *Invest Ophthalmol Vis Sci*. 2002;43:3480–3488.
54. Lewis GP, Linberg KA, Geller SF, et al. Effects of the neurotrophin brain-derived neurotrophic factor in an experimental model of retinal detachment. *Invest Ophthalmol Vis Sci*. 1999;40:1530–1544.
55. Lewis G, Mervin K, Valter K, et al. Limiting the proliferation and reactivity of retinal Muller cells during experimental retinal detachment: the value of oxygen supplementation. *Am J Ophthalmol*. 1999;128:165–172.
56. Mervin K, Valter K, Maslim J, et al. Limiting photoreceptor death and deconstruction during experimental retinal detachment: the value of oxygen supplementation. *Am J Ophthalmol*. 1999;128:155–164.
57. Sakai T, Lewis GP, Linberg KA, et al. The ability of hyperoxia to limit the effects of experimental detachment in cone-dominated retina. *Invest Ophthalmol Vis Sci*. 2001;42:3264–3273.